

Extremely high efficient coupling between long range surface plasmon polariton and dielectric waveguide mode

Fang Liu,^{1,a)} Ruiyuan Wan,¹ Yunxiang Li,¹ Yidong Huang,^{1,b)} Yoshikatsu Miura,² Dai Ohnishi,² and Jiangde Peng¹

¹Department of Electronic Engineering, State Key Laboratory of Integrated Optoelectronics, Tsinghua University, Beijing 100084, People's Republic of China

²Photonics R&D Center, ROHM Co., Ltd., Kyoto 615-8585, Japan

(Received 31 May 2009; accepted 31 July 2009; published online 3 September 2009)

To connect the surface plasmon polariton (SPP) based devices with the conventional dielectric devices is a significant issue for the further development of SPP and related applications. In this paper, extremely high efficient coupling ($>99\%$) between long range SPP (LRSPP) waveguide mode and TM mode of dielectric waveguide has been demonstrated from a hybrid coupler, which composed of an Au (LRSPP) waveguide and a SiN (dielectric) waveguide. Based on this hybrid coupler, a polarization splitter with pure TM mode output from one arm and TE mode output from the other arm with high TE/TM extinction ratio has been realized. © 2009 American Institute of Physics. [DOI: 10.1063/1.3212145]

Surface plasmon polariton (SPP) is a kind of transverse-magnetic (TM) surface electromagnetic excitation that propagates in a wavelike fashion along the interface between metal and dielectric medium.^{1,2} It has shown the unique characteristics and potential applications on integrated optical circuit, sensing, optical storage, and so on.³⁻⁹ Compared with general SPP, the long range SPP (LRSPP) mode has much lower loss^{10,11} and is more sensitive to the refractive index of the dielectric medium surrounding the metal surfaces.^{12,13} Based on these characteristics, the LRSPP related devices, such as splitter, modulator, and sensor have been reported.¹⁴⁻¹⁷

Recently, a kind of hybrid coupler composed of a LRSPP waveguide and dielectric waveguide(s) has been proposed by our group. It has been predicted theoretically that high efficient coupling can occur between the LRSPP waveguide mode and the dielectric waveguide modes.^{18,19} This kind of coupling between different waveguides is very significant because it could not only provide an effective approach to connect the LRSPP devices with dielectric devices, but also realize a novel LRSPP-dielectric hybrid device, which possess the advantages of both LRSPP and existing dielectric devices.

This paper reports the experimental results on the hybrid coupler composed of an Au strip and a SiN strip embedded in SiO₂. Extremely high efficient coupling ($>99\%$) between LRSPP waveguide mode and TM mode of the SiN waveguide has been demonstrated, which is much higher than that reported in Ref. 20. Due to the different coupling characteristics for TM and TE mode, a polarization splitter with pure TM mode output from Au waveguide and TE mode output from SiN waveguide with TE/TM extinction ratio of 24 dB has been realized.

Figure 1(a) shows the structure of the hybrid coupler schematically. The Au strip (yellow) and SiN strip (gray) are embedded horizontally in the SiO₂. The length of the hybrid

coupler is L . The cross section of the coupler with detailed structure parameters are shown in the inset.

To fabricate the hybrid coupler, a Si wafer covered by a 15 μm thick SiO₂ layer (with refractive index $n_{\text{sub}}=1.446$) was selected as the substrate. On the substrate, 1 μm thick SiO₂ ($n_b=1.453$) layer and $T_d=32$ nm thick SiN ($n_d=1.871$) layer were prepared successively by sputtering and plasma-enhanced chemical-vapor deposition (PECVD), respectively. By adopting standard UV lithography, photoresist strip pattern was formed on the SiN layer with width of $W_d=6$ μm . After dry etching process by reactive ion etching and removing the photoresist, a 6 μm wide SiN waveguide on SiO₂ layer was fabricated. The next step was to fabricate the $W_m=8$ μm wide and $T_m=12$ nm thick Au strip by cover lithography, Au magnetic sputtering, and lift off process with the help of the photoresist remover. Here, the cover lithog-

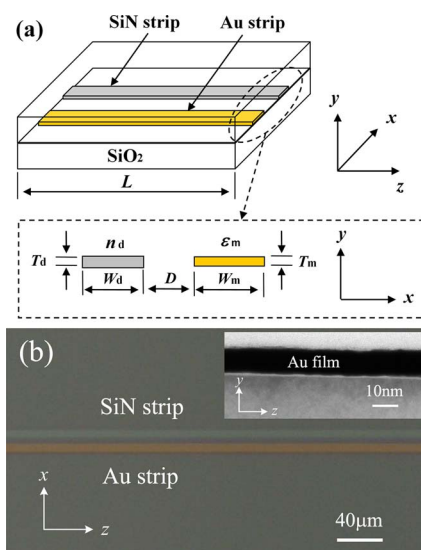


FIG. 1. (Color online) (a) Schematic structure of the hybrid coupler with Au strip (yellow) and SiN strip (gray) surrounded by SiO₂. Inset is the cross section of the structure in the x - y plane. (b) Photo of the hybrid coupler under microscope. Inset is the photo of the Au film by transmission electron microscope.

^{a)}Electronic mail: liu_fang@tsinghua.edu.cn.

^{b)}Electronic mail: yidonghuang@tsinghua.edu.cn.

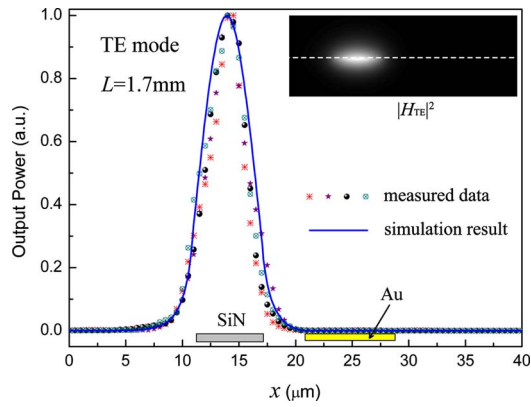


FIG. 2. (Color online) TE mode output power profile along x axis measured from four samples when input was fixed at $\lambda_0=1.55 \mu\text{m}$ and applied on the SiN waveguide. The inset is the simulated 2D TE output energy profile in the x - y plane. The solid line illustrates the simulated optical power received by the tapered fiber with $1 \mu\text{m}$ mode size along the white dashed line marked in the inset.

raphy, which was to fabricate the concave photoresist strip by adopting the UV lithography again, was very important to make sure that the Au strip (concave photoresist strip) was parallel to the SiN waveguide and meanwhile control the distance D between these two different arms as $4 \mu\text{m}$. At last, as the cover layer on the SiN and the Au strip, another $1 \mu\text{m}$ thick SiO_2 ($n_b=1.453$) was sputtered and $9 \mu\text{m}$ thick SiO_2 ($n_{\text{sup}}=1.448$) was deposited by PECVD successively. The two $1 \mu\text{m}$ thick SiO_2 layers prepared by sputtering were to make sure that the refractive index of the dielectrics above and beneath the Au strip are almost the same. Figure 1(b) shows the photo of the hybrid coupler under microscope. To realize the high efficient coupling between the two different waveguides, the sputtering speed of Au was controlled as 2–3 nm/min for exact Au waveguide thickness. The 10 nm level Au film was observed by the transmission electron microscope and the photo is shown as the inset of Fig. 1(b).

After the fabrication processes, the hybrid coupler was cut into several samples with different length L . The measurement system for coupling characteristics includes a tunable laser (1350–1630 nm), a polarization controller, an input tapered lens fiber, a precise fiber alignment system, an output tapered lens fiber, and a power meter. The polarization controller was used here to control the polarization (TM and TE) of the input light to investigate the coupling characteristics for different polarizations.

First, setting the wavelength of input light at $\lambda_0=1.55 \mu\text{m}$ and switching the polarization to TE mode, the field profile at the output end of the hybrid coupler was measured by fixing the input fiber to the center of the SiN waveguide at one end and scanning the output fiber along x axis at the other end. Figure 2 shows the measurement results of four samples with different marks when $L=1.7 \text{ mm}$ and the corresponding simulation result of two-dimensional (2D) TE output power profile is obtained by calculating the coupled eigenmodes of the hybrid coupler with finite element method and then expanding the input by the coupled eigenmodes to study the coupling questions.¹⁸ It can be seen that the measurement results are well fit by the solid line of the simulation result, which illustrates the optical power received by the tapered fiber with $1 \mu\text{m}$ mode size along the white dashed line marked in the inset. It can be noticed that no TE output can be detected from the Au strip, which is consistent

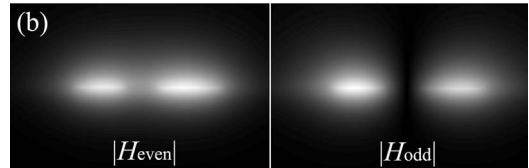
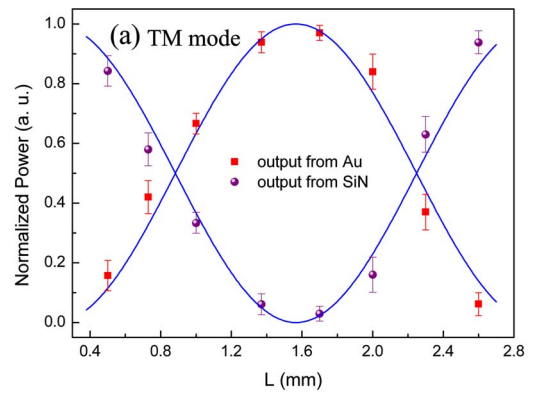


FIG. 3. (Color online) (a) TM output power from Au strip (square) and SiN strip (dot) normalized by the total output with various interaction lengths when input was fixed at $\lambda_0=1.55 \mu\text{m}$ and applied on the SiN waveguide. The measured data are well fitted by the solid curves of $\sin^2(\kappa L)$. (b) The amplitude of magnetic field $|H|$ of the two simulated TM eigenmodes.

with our theoretical prediction, namely TE mode cannot couple to the LRSPP waveguide mode.¹⁸ Similar measurement results were obtained for the samples with different length and different input wavelength. The measured loss of TE mode is about 0.23 dB/mm. Compared with the simulated value of 0.083 dB/mm, the higher loss may mainly result from the imperfect fabrication of the SiN strip.

When TM mode was applied on the SiN waveguide at the wavelength of $\lambda_0=1.55 \mu\text{m}$, the output power distribution changed dramatically. The output power can be detected from not only the SiN waveguide but also the Au waveguide. Figure 3(a) shows the normalized output power coupled to the Au waveguide (square) and remained in the SiN waveguide (dot) with different interaction length L from 0.5 to 2.6 mm. The measured power at the output end of both waveguides are well fitted by the solid curves of $\sin^2(\kappa L)$, where $\kappa=k_0 \times \Delta n_{\text{eff}}$ and $\Delta n_{\text{eff}}=|n_e-n_o|$ is the effective refractive index difference between the even and odd modes, as shown in Fig. 3(b). Theoretical analysis indicates that the energy transfer between two different waveguides results from the existence of the two coupled eigenmodes (even and odd mode) and their different effective refractive index.¹⁸ The high symmetry of the eigenmodes shown in Fig. 3(b) means the high coupling efficiency between LRSPP and dielectric waveguide modes.

Figures 4(a) and 4(b) show the output power distribution along x axis measured for the samples with $L=0.7$ and 1.7 mm , respectively. The simulation results of 2D output power profile of the TM mode are also shown in the inset of Fig. 4, like that of the TE mode in Fig. 2. The measured data are well fit by the solid lines, which illustrate the simulated optical power received by the tapered fiber along the white dashed line marked in the corresponding inset. For the case of $L=0.7 \text{ mm}$, almost 40% of the energy couples from SiN waveguide to Au (LRSPP) waveguide, while when $L=1.7 \text{ mm}$, 98% of the energy couples to the Au waveguide with little energy remaining in the input SiN waveguide. For the hybrid coupler with $L=1.7 \text{ mm}$, the TM loss is about

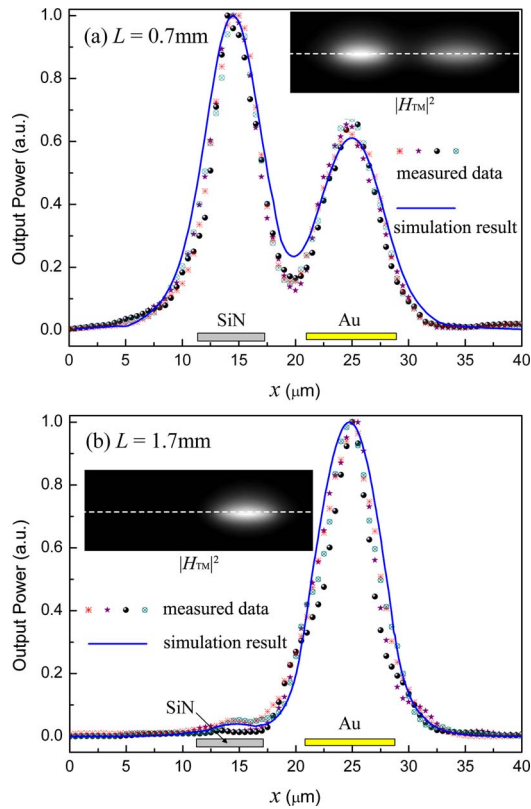


FIG. 4. (Color online) TM mode output power profile of four samples along x axis with reaction length (a) $L=0.7$ mm, (b) $L=1.7$ mm, where the input was applied on the SiN waveguide with $\lambda_0=1.55$ μm . The inset is the corresponding simulated 2D TM output power profile in the x - y plane. The simulated optical power received by the tapered fiber with 1 μm mode size along the white dashed line in the inset is well fit to the measured data.

1.26 dB, which is much higher than the simulated value of 0.288 dB and could be reduced by improving the fabrication technique.

For the sample with length $L=1.7$ mm, the proportion of the TM mode coupled to the Au strip (square) and that remained in SiN waveguide (dot) were measured by scanning the wavelength λ_0 from 1.425 to 1.625 μm , as shown in Fig. 5. An extremely high coupling efficiency, as high as 99.75%, was observed at the wavelength of $\lambda_0=1.485$ μm , which is higher than that measured at $\lambda_0=1.55$ μm . The solid line is the simulation result, which is almost consistent with the measurement results. It can be seen that the coupling efficiency is higher than 99% for the wavelength range

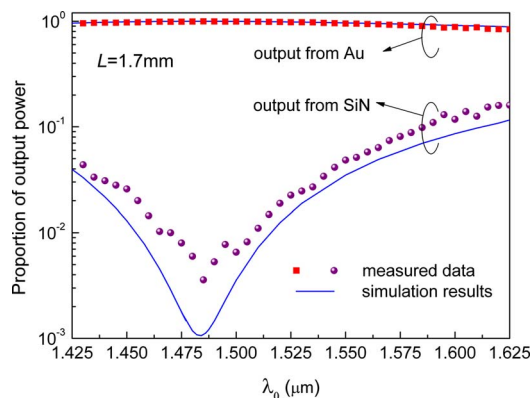


FIG. 5. (Color online) Proportion of the TM power coupled to Au strip (square) and that remained in SiN waveguide (dot) as a function of wavelength when $L=1.7$ mm. The solid line is the simulation results.

from 1.465 to 1.510 μm . The wavelength corresponding to the highest coupling efficiency could be moved to 1.55 μm by adjusting the structure parameters.

Considering the above measurement results, it is easy to notice that the coupling characteristics are quite different between TE and TM mode. Therefore, a high performance polarization splitter can be realized. Pure TM mode without any noise of TE mode can always be obtained from Au strip for different wavelengths. And the TE mode output with high TE/TM extinction ratio, as high as 24 dB, was derived from the SiN waveguide. Our further theoretical study also shows that the coupling characteristics between LRSP mode and dielectric waveguide mode is rather sensitive to the dielectric refractive index on metal surface, which is promising for a high sensitive refractive index sensor and optical intensity modulator with very low driving power.²¹

In conclusion, a hybrid coupler, with a thin Au (LRSP) waveguide and a SiN (dielectric) waveguide embedded in SiO₂, has been fabricated. Extremely high efficient coupling (>99%) between LRSP waveguide mode and TM polarized dielectric waveguide mode has been observed. Based on this hybrid coupler, a polarization splitter with pure TM mode output from Au waveguide and a TE mode output with high TE/TM extinction ratio of 24 dB from SiN waveguide has been realized. Furthermore, other functional devices, such as sensor and modulator, could also be derived.

This work is supported by the National Basic Research Program of China (973 Program) under Contract No. 2007CB307004 and the National Natural Science Foundation of China (Grant Nos. NSFC-60537010 and NSFC-60877023). The authors would like to thank Professor Wei Zhang and Dr. Xue Feng and Kaiyu Cui of Tsinghua University for their valuable discussions and helpful comments.

¹H. Raether, *Surface Plasmons* (Springer, Berlin, 1988).

²A. V. Zayats, I. I. Smolyaninov, and A. A. Maradudin, *Phys. Rep.* **408**, 131 (2005).

³W. L. Barnes, A. Dereux, and T. W. Ebbesen, *Nature (London)* **424**, 824 (2003).

⁴E. Ozbay, *Science* **311**, 189 (2006).

⁵S. I. Bozhevolnyi, V. S. Volkov, E. Devaux, J. Y. Laluet, and T. W. Ebbesen, *Nature (London)* **440**, 508 (2006).

⁶X. D. Hoa, A. G. Kirk, and M. Tabrizian, *Biosens. Bioelectron.* **23**, 151 (2007).

⁷P. Berini, *New J. Phys.* **10**, 105010 (2008).

⁸N. Fang, H. Lee, C. Sun, and X. Zhang, *Science* **308**, 534 (2005).

⁹X. Luo and T. Ishihara, *Appl. Phys. Lett.* **84**, 4780 (2004).

¹⁰P. Berini, *Phys. Rev. B* **61**, 10484 (2000).

¹¹T. Nikolajsen, K. Leosson, I. Salakhutdinov, and S. I. Bozhevolnyi, *Appl. Phys. Lett.* **82**, 668 (2003).

¹²I. Breukelaar, R. Charbonneau, and P. Berini, *J. Appl. Phys.* **100**, 043104 (2006).

¹³G. G. Nenninger, P. Tobisika, J. Homola, and S. S. Yee, *Sens. Actuators B* **74**, 145 (2001).

¹⁴R. Charbonneau, C. Scales, I. Breukelaar, S. Fafard, N. Lahoud, G. Mattiussi, and P. Berini, *J. Lightwave Technol.* **24**, 477 (2006).

¹⁵A. Boltasseva, T. Nikolajsen, K. Leosson, K. Kjaer, M. S. Larsen, and S. I. Bozhevolnyi, *J. Lightwave Technol.* **23**, 413 (2005).

¹⁶T. Nikolajsen, K. Leosson, and S. I. Bozhevolnyi, *Appl. Phys. Lett.* **85**, 5833 (2004).

¹⁷R. Slavik and J. Homola, *Sens. Actuators B* **123**, 10 (2007).

¹⁸F. Liu, Y. Rao, Y. Huang, W. Zhang, and J. Peng, *Appl. Phys. Lett.* **90**, 141101 (2007).

¹⁹F. Liu, Y. Rao, X. Tang, R. Wan, Y. Huang, W. Zhang, and J. Peng, *Appl. Phys. Lett.* **90**, 241120 (2007).

²⁰A. Degiron, S. Y. Cho, T. Tyler, N. M. Jokerst, and D. R. Smith, *New J. Phys.* **11**, 015002 (2009).

²¹F. Liu, R. Wan, Y. Huang, and J. Peng, *Opt. Lett.* **34**, 2697 (2009).